Cheng *et al. Chem Synth* 2023;3:13
DOI: 10.20517/cs.2022.43

Chemical Synthesis

Research Article

Open Access

Dedicated to Professor Alain Krief on the occasion of his 80th Birthday

Luminescent alkynylplatinum(II) terpyridine-containing conjugated polymers: synthesis, characterization and photophysical studies

Heung-Kiu Cheng, Vivian Wing-Wah Yam*

Institute of Molecular Functional Materials and Department of Chemistry, The University of Hong Kong, Hong Kong 999077, China.

***Correspondence to:** Prof. Vivian Wing-Wah Yam, Institute of Molecular Functional Materials and Department of Chemistry, The University of Hong Kong, Pokfulam Road, Hong Kong 999077, China. E-mail: wwyam@hku.hk

How to cite this article: Cheng HK, Yam VWW. Luminescent alkynylplatinum(II) terpyridine-containing conjugated polymers: synthesis, characterization and photophysical studies. *Chem Synth* 2023;3:13. https://dx.doi.org/10.20517/cs.2022.43

Received: 29 Dec 2022 **First Decision:** 2 Feb 2023 **Revised:** 17 Feb 2023 **Accepted:** 23 Feb 2023 **Published:** 9 Mar 2023

Academic Editor: Bao-Lian Su **Copy Editor:** Ke-Cui Yang **Production Editor:** Ke-Cui Yang

Abstract

A series of alkynylplatinum(II) terpyridine complexes and alkynylplatinum(II) terpyridine-containing conjugated polymers with different polymer backbones has been synthesized, and their spectroscopic properties and Förster resonance energy transfer (FRET) processes has been investigated. The platinum(II)-containing polymers exhibit dual emissive features with emission maxima at *ca.* 416-465 nm and *ca.* 671-673 nm, which are assigned to be originated from singlet intraligand (^{1}IL) excited states from the polymer backbone and triplet metal-metal-to-ligand charge transfer (^{3}MMLCT) excited states from the platinum(II) pendants, respectively. The Förster radii (R_0) of the platinum(II)-containing conjugated polymers have been determined, and their distinctive thermo-responsive luminescence changes have also been observed. The present work has demonstrated the utilization of "click" reaction for the preparation of platinum(II)-containing conjugated polymers, which show unique photophysical and spectroscopic properties. Through the judicious design, this type of platinum(II)-containing polymer is found to be sensitive to temperature, resulting in ratiometric emission changes. This study has provided valuable insights into the preparation of metal-containing polymeric systems for different applications.

Keywords: Platinum(II) complexes, conjugated polymers, FRET

INTRODUCTION

Over the past few decades, conjugated polymers, which have been extensively studied with well-known examples such as poly(*p*-phenylene vinylene) (PPV)[1], polypyrrole (PPy)[2-4], polythiophene (PT)[5] and so on, represent important classes of organic macromolecules, and have found widespread applications in organic photovoltaic devices, light-emitting diodes, sensing materials, and others[6-11]. The prominence of conjugated polymers can be attributed to their unique properties of high planarity and extended π-electron delocalization, empowering them with rich photophysical and electrochemical functionalities for specific applications[6-11]. After the success in designing and synthesizing different kinds of conjugated polymers, attempts have been made to integrate conjugated polymers with transition metals, namely metallo-conjugated polymers, with a view to not only improving the physical properties of the parent organic polymers such as mechanical strength, thermal stability and carrier mobility but also enriching their photophysical properties such as harvesting energy from the triplet excited state and extending the absorption spectrum to the red or near-infrared (NIR) region[12-19]. Earlier examples include ruthenium(II)-containing conjugated polymers with poly(bpy-*co*-benzobisoxazole)s or poly(bpy-*co*-benzobisthiazole)s as the polymer backbones[20] and iridium(III)-containing conjugated polymers with polyfluorene as the polymer backbone and carbazole unit as the pendant[21]. Unlike most other commonly studied transition metal centers, including ruthenium(II), rhodium(III) and iridium(III), d^8 platinum(II) center favors coordination of a square-planar geometry, and their complexes, especially those bearing conjugated aromatic ligands capable of exhibiting π-π interactions, are well-known for their ability to self-assemble[22-26], forming aggregates[27-31] and providing remarkable photophysical properties associated with Pt···Pt and π-π interactions[32-35]. In light of their supramolecular assembly capability, it is envisaged that the introduction of platinum centers into conjugated polymers may provide an opportunity to further modulate the photophysical and morphological properties of the resulting metal–organic hybrid materials[36-38]. Although there were examples of platinum(II)-containing conjugated polymers such as platinum(II) polyynes[39-46] and cyclometalating bidentate ligand-containing platinum(II)-based conjugated polymers[47-49], none of these examples demonstrates supramolecular assembly properties or utilizes the system of tridentate *N*-donor ligands. In this work, a series of alkynylplatinum(II) terpyridine complexes (**1** and **2**) and alkynylplatinum(II) terpyridine-containing conjugated polymers with different polymer backbones (**3**-**5**) [Scheme 1] has been synthesized and their photophysical properties as well as FRET processes have been studied. With the aid of various spectroscopic techniques, the photophysical and spectroscopic properties of the organic polymers, platinum(II) precursor complexes and the newly synthesized platinum(II)-containing conjugated polymers have been investigated systematically. It was found that the choice of the polymer backbones would influence the intramolecular FRET efficiencies of the system of platinum(II)-containing polymers. Through the understanding of different factors affecting the spectroscopic properties and FRET processes of the platinum(II)-containing polymers, it is envisaged that the present study can provide further insights into the design and development of metal-containing polymers for the construction of different functional materials.

EXPERIMENTAL

Syntheses of conjugated polymers and complexes 1-5

The synthetic routes for platinum (II) precursor and reference complex are depicted in Supplementary Scheme 1. Alkynylplatinum (II) terpyridine precursor **1** for "click" reaction was prepared based on a modified procedure of copper(I)-catalyzed dehalogenation reaction (pp 9, Supplementary Materials)[50]. The alkynylplatinum (II) terpyridine reference complex **2** was obtained through copper(I)-catalyzed alkyne-azide cycloaddition ("click" reaction) by reacting **1**, 1-azidohexane, CuBr, PMDETA and sodium ascorbate in a saturated solution of ammonium triflate in DMF (pp S10, Supplementary Materials). **1** and **2** were obtained as orange and red solid, respectively. These complexes are found to be highly soluble in organic solvents such as dichloromethane, chloroform, acetone, methanol, THF, and others.

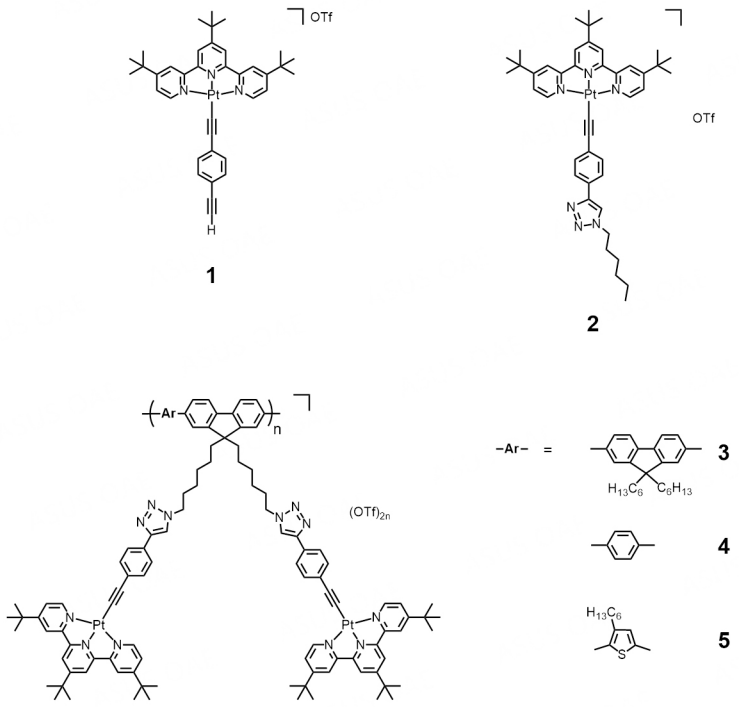

Scheme 1. Molecular structures of the platinum(II) complexes (**1** and **2**) and the platinum(II)-containing conjugated polymers (**3**-**5**).

The synthetic routes for the conjugated polymers are depicted in Supplementary Scheme 2. Detailed syntheses of the bromo-containing conjugated polymers, poly[fluorene($C_6H_{12}Br$)$_2$-*co*-fluorene(C_6H_{13})$_2$] (**PF-Br**), poly[fluorene($C_6H_{12}Br$)$_2$-*co*-phenylene](**PFP-Br**) and poly[fluorene($C_6H_{12}Br$)$_2$-*co*-thiophene(C_6H_{13})] (**PFT-Br**), and the corresponding azido-containing conjugated polymers (**PF-N$_3$**, **PFP-N$_3$** and **PFT-N$_3$**) are shown in pp S11-S14, Supplementary Materials. All the organic conjugated polymers were found to have good solubility in organic solvents such as chlorinated solvents, toluene, THF, and others. The identities of all of the organic conjugated polymers have been confirmed by ^{1}H NMR spectroscopy and GPC analysis.

The synthetic routes for the platinum(II)-containing conjugated polymers are depicted in Supplementary Scheme 3. The platinum(II)-containing conjugated polymers **3**-**5** were also obtained through copper(I)-catalyzed alkyne-azide cycloaddition of the corresponding azido-containing conjugated polymers and **1** in THF-DMF mixture in the presence of ammonium triflate (pp S15-S17, Supplementary Materials). The products were purified by precipitation in deionized water containing ammonium triflate. The platinum(II)-containing conjugated polymers were found to have fair solubility in acetonitrile, DMF and DMSO. Their limited solubility in methanol and THF has facilitated the purification by washing the precipitate with methanol and THF to further remove any unreacted starting materials.

Characterization

All the newly synthesized platinum(II) complexes **1** and **2** and platinum(II)-containing polymers **3**-**5** have been characterized by ^{1}H NMR and IR spectroscopy. In addition, **1** and **2** were also confirmed by positive-ion FAB mass spectrometry and showed satisfactory results in the elemental analyses. **3**-**5** were also confirmed by GPC analysis using DMF with 0.1 M KPF_6 as eluent. Representative GPC data of **5** is provided in Supplementary Figure 1.

From the IR measurements of **3-5** [Supplementary Figures 2-4], the disappearance of the strong absorption of the N=N=N stretch of the azide precursor at *ca.* 2095 cm^{-1}, the appearance of weak absorption of the C≡C stretch at 2110 cm^{-1} and strong absorption of the triflate counter-ion at *ca.* 1155 and 1030 cm^{-1} indicated the successful incorporation of the platinum(II) complexes onto the polymer *via* "click" reaction.

RESULTS AND DISCUSSION

The polymers, **PF-Br**, **PFP-Br** and **PFT-Br**, are soluble in dichloromethane and give high-energy absorption bands with a peak maxima at *ca.* 375-398 nm [Supplementary Figure 5 and Supplementary Table 1], which are assigned as the π→π* transitions along the polymer backbone, while these polymers show strong vibronic-structured emissions with peak maxima at *ca.* 410-462 nm upon photoexcitation [Supplementary Figures 6-9 and Supplementary Table 2], which are assigned as the singlet [π→π*] fluorescence of the conjugated polymer backbone.

For complexes **1-5**, they all give pale yellow solutions in acetonitrile. Their corresponding UV-vis absorption data and spectra in acetonitrile at 298 K are depicted in Table 1 and Figure 1, respectively. All the complexes exhibit intense absorption bands at *ca.* 285-341 nm with molar extinction coefficients in the order of 10^4 dm^3 mol^{-1} cm^{-1} and less intense low-energy absorption bands at *ca.* 420-466 nm with molar extinction coefficients in the order of 10^3 dm^3 mol^{-1} cm^{-1}. The higher-energy bands are ascribed to intraligand (IL) [π→π*] transitions of alkynyl and terpyridine ligands, while the lower-energy bands are assigned as an admixture of metal-to-ligand charge transfer (MLCT) [dπ(Pt)→π*(tpy)] and ligand-to-ligand charge transfer (LLCT) [π(alkynyl)→π*(tpy)] transitions. For the platinum(II)-containing conjugated polymers **3-5**, intense absorption bands at *ca.* 374-409 nm have been observed. With reference to the previous studies on the conjugated polymers[51-54] and the UV-vis absorption studies of the corresponding organic polymers [Supplementary Figure 5], these absorptions are tentatively assigned as the IL [π→π*] transitions of the polymer backbones. Interestingly, the lower-energy bands of **3-5** are extended to longer wavelengths when compared to the reference complex **2**. Since the molecular structures of the platinum(II) pendants in **3-5** are the same as that in **2**, the further red-shifted absorption tails suggest the existence of metal-metal-to-ligand charge transfer (MMLCT) character. As such, concentration-dependent UV-vis absorption studies have been performed. Based on the spectra [Supplementary Figures 10-14], the precursor platinum(II) complexes **1** and **2** and the platinum(II)-containing conjugated polymers **3-5** show good agreement with Beer's Law, suggesting that there are no significant intermolecular self-assembly properties of **1-5** upon increasing the concentration. However, the intramolecular self-assembly mode of having two platinum(II) pendants in each repeating unit, which are stabilized by the presence of intramolecular Pt···Pt and π-π interactions, may explain the presence of low-energy MMLCT bands for the platinum(II)-containing conjugated polymers **3-5**. In this regard, temperature-dependent UV-vis absorption experiments for **3-5** have been carried out. From the spectra [Figures 2-4], the low-energy band at *ca.* 450 nm shows a drop in absorbance accompanied by a blue shift of the high-energy band at *ca.* 400 nm upon increasing temperature, suggesting the occurrence of deaggregation process of both the platinum(II) terpyridine moieties and the polymer backbones, which corroborates with the disruption of intramolecular Pt···Pt and π-π interactions at high temperatures.

Complexes **1** and **2** are found to give phosphorescence in degassed solutions, while dual-emissive behaviors have been observed for the platinum(II)-containing conjugated polymers **3-5** in degassed solutions upon excitation. The luminescence data of all complexes have been summarized in Table 2. Upon photoexcitation at λ > 350 nm, **1** and **2** show Gaussian-shape emission bands centered at 596 nm and 630 nm in degassed acetonitrile [Supplementary Figure 15]. The large Stokes shifts and the long emission lifetimes in the microsecond regime indicate that these emissions are originated from a triplet parentage. Together with the

Table 1. UV-Vis absorption data for 1-5 at 298 K

Complex	Medium	Absorption λ/nm (ε/dm^3 mol^{-1} cm^{-1})
[Pt(^{t}Bu$_3$tpy)(C≡CC$_6$H$_4$C≡CH)]OTf (**1**)	CH_3CN	285 (52,030), 322 (18,620), 338 (19,130), 420 (6,660)
[Pt(^{t}Bu$_3$tpy)(C≡CC$_6$H$_4$C$_2$HN$_3$C$_6$H$_{13}$)]OTf (**2**)	CH_3CN	287 (49,290), 305 sh (35,150), 324 sh (16,330), 338 (15,980), 401 sh (15,980), 434 (5,560)
[PF-{N$_3$C$_2$H-C$_6$H$_4$C≡CPt(^{t}Bu$_3$tpy)}$_2$](OTf)$_{2n}$ (**3**)[a]	CH_3CN	288 (71,290), 308 sh (55,900), 341 (37,020), 383 (48,560), 445 sh (8,010)
[PFP-{N$_3$C$_2$H-C$_6$H$_4$C≡CPt(^{t}Bu$_3$tpy)}$_2$](OTf)$_{2n}$ (**4**)[a]	CH_3CN	287 (69,780), 308 sh (57,730), 341 (38,350), 374 (41,140), 451 sh (8,190)
[PFT-{N$_3$C$_2$H-C$_6$H$_4$C≡CPt(^{t}Bu$_3$tpy)}$_2$](OTf)$_{2n}$ (**5**)[a]	CH_3CN	289 (64,250), 308 sh (50,700), 340 sh (25,560), 409 (33,250), 466 sh (8,320)

[a]The molar extinction coefficients of the metallopolymers were approximated per repeating unit.

Table 2. Emission data for 1-5

Complex	Medium (T/K)	λ_{em}/nm (τ_o/μs)	Φ_{lum}[a]
[Pt(^{t}Bu$_3$tpy)(C≡CC$_6$H$_4$C≡CH)]OTf (**1**)	CH_3CN (298)	596 (1.09)	5.0 × 10^{-2b}
[Pt(^{t}Bu$_3$tpy)(C≡CC$_6$H$_4$-C$_2$HN$_3$C$_6$H$_{13}$)]OTf (**2**)	CH_3CN (298)	630 (0.14)	8.5 × 10^{-3b}
[PF-{N$_3$C$_2$H-C$_6$H$_4$C≡C-Pt(^{t}Bu$_3$tpy)}$_2$](OTf)$_{2n}$ (**3**)	CH_3CN (298)	416[c] (< 0.1), 671 (0.14)	1.2 × 10^{-3d} 2.6 × 10^{-3b}
[PFP-{N$_3$C$_2$H-C$_6$H$_4$C≡C-Pt(^{t}Bu$_3$tpy)}$_2$](OTf)$_{2n}$ (**4**)	CH_3CN (298)	417[c] (< 0.1), 673 (0.70)	9.0 × 10^{-4d} 1.4 × 10^{-2b}
[PFT-{N$_3$C$_2$H-C$_6$H$_4$C≡C-Pt(^{t}Bu$_3$tpy)}$_2$](OTf)$_{2n}$ (**5**)	CH_3CN (298)	465[c] (< 0.1), 673 (0.66)	8.4 × 10^{-4d} 1.7 × 10^{-3b}

[a]Data obtained with an uncertainty of 10 %; [b]the relative luminescence quantum yields were measured at room temperature using [Ru(bpy)$_3$]Cl$_2$ in degassed acetonitrile as a standard; [c]vibronic-structured band with vibrational progressional spacings of *ca.* 1150-1320 cm^{-1}; [d]the relative luminescence quantum yields were measured at room temperature using quinine sulfate in 0.5 M H_2SO_4 as a standard.

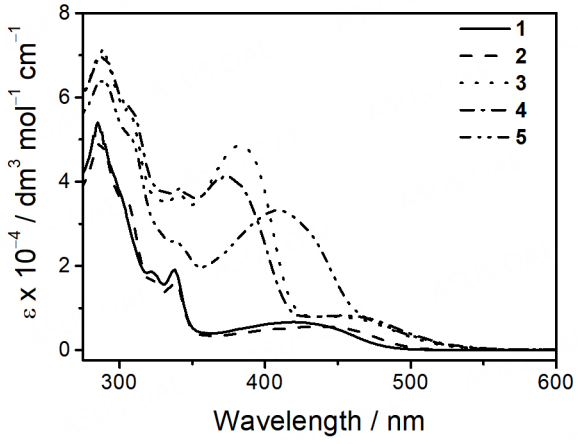

Figure 1. UV-Vis absorption spectra of **1-5** in acetonitrile at 298 K.

relatively short photoluminescence lifetimes in the range of 1 ms or lower, these emission bands are assigned to be originated from admixtures of ^{3}MLCT [dπ(Pt)→π(tpy)] and ^{3}LLCT [π(alkynyl)→π*(tpy)] excited states. On the other hand, platinum(II)-containing conjugated polymers **3-5** exhibit dual-emissive behaviors upon excitation [Figure 5]. The high-energy emission bands are vibronic-structured with emission maxima at *ca.* 416-465 nm, while the low-energy emissions are of Gaussian shape and centered at *ca.* 672 nm. Based on the previous studies[51-54] and the corresponding emission measurements of the organic

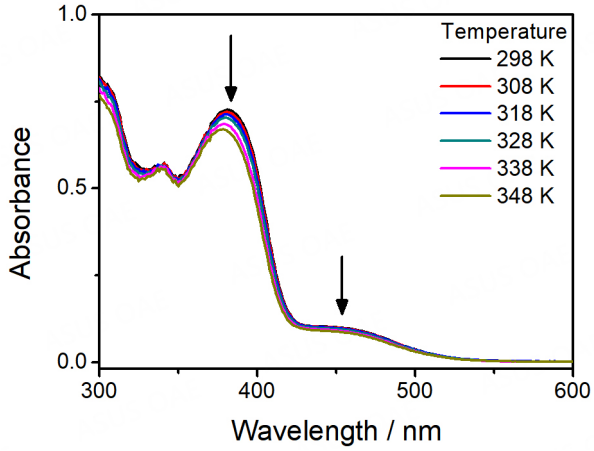

Figure 2. UV-Vis absorption spectral changes of [PF-{N_3C_2H-$C_6H_4C{\equiv}CPt(^tBu_3tpy)$}$_2$](OTf)$_{2n}$ (**3**) in acetonitrile with increasing temperature.

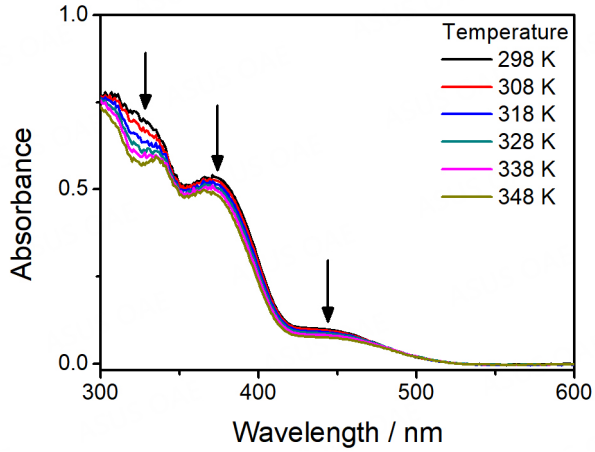

Figure 3. UV-Vis absorption spectral changes of [PFP-{N_3C_2H-$C_6H_4C{\equiv}CPt(^tBu_3tpy)$}$_2$](OTf)$_{2n}$ (**4**) in acetonitrile with increasing temperature.

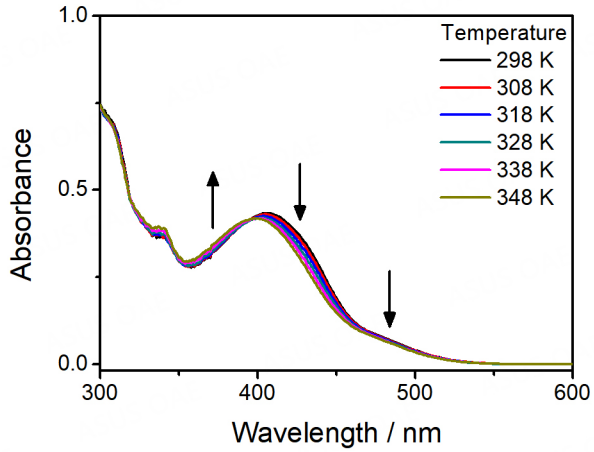

Figure 4. UV-Vis absorption spectral changes of [PFT-{N_3C_2H-$C_6H_4C{\equiv}CPt(^tBu_3tpy)$}$_2$](OTf)$_{2n}$ (**5**) in acetonitrile with increasing temperature.

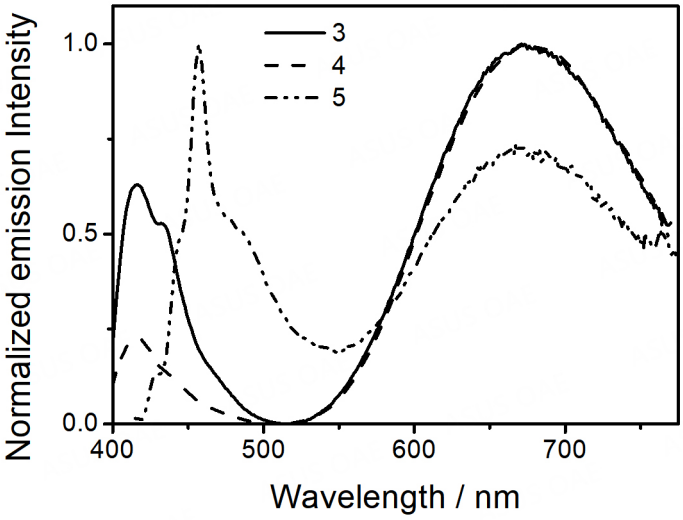

Figure 5. Normalized emission spectra of **3-5** in degassed acetonitrile at 298 K.

conjugated polymers, the high-energy emissions are ascribed to the singlet [$\pi\rightarrow\pi^*$] excited state of the polymer backbone, while the low-energy emissions of **3-5** are tentatively assigned to be originated from the ^{3}MMLCT excited states. To further validate the ^{3}MMLCT origin of these low-energy emissions, temperature-dependent emission studies have been performed [Supplementary Figures 16-18]. As a result, **3-5** exhibit a decrease in intensity of the low-energy emissions with significant blue shifts upon increasing temperature.

On the other hand, distinctive thermo-responsive emission changes have also been observed for the platinum(II)-containing conjugated polymers **3-5**. Upon increasing the temperature of the solution of **3**, the high-energy emission from the polymer backbone is found to increase in intensity [Figure 6]. The reason behind this can be attributed to the decrease in FRET efficiency from the polymer backbone to the platinum(II) moieties. From the variable-temperature UV-vis absorption spectral traces of **3** [Figure 2], there is a decrease in absorbance of the MMLCT band upon increasing temperature, leading to a decrease in the spectral overlap and the enhanced recovery of the polymer fluorescence [Figure 6]. Moreover, **4** is found to exhibit the largest recovery of the high-energy emission when compared to others upon increasing temperature, as shown in Figure 7. Since **4** bears the least number of alkyl chains in each repeating unit, it is believed that the energy would be less effectively dissipated through non-radiative decay pathways. As a result, the FRET process dominates in **4**, resulting in the greatest recovery of the polymer backbone emission. Furthermore, both emission bands of **5** are found to be diminished with increasing temperature [Figure 8], which can be attributed to the more dominating non-radiative process when compared to the recovery of the fluorescence of the polymer backbone. The corresponding ratiometric emission intensity plots of **3-5** have been depicted in Figure 9.

Due to the good spectral overlap between the absorption spectrum of the reference complex **2** and the emission spectra of the conjugated polymers (**PF-Br**, **PFP-Br** and **PFT-Br**) [Figure 10], it is believed that the intramolecular FRET process from the polymer backbone to the platinum(II) pendant would likely occur upon photoexcitation. Although the emissions from the conjugated polymer backbones could still be observed for **3-5**, they are already effectively quenched when compared to their corresponding organic polymers (Φ_{lum} of **PF-Br**, **PFP-Br** and **PFT-Br** = 0.45-0.92; Φ_{lum} of **3-5** = 8.4×10^{-4}-1.2×10^{-3}). It is worth noting that different extents of quenching efficiencies have been observed for **3-5**. For example, the emission

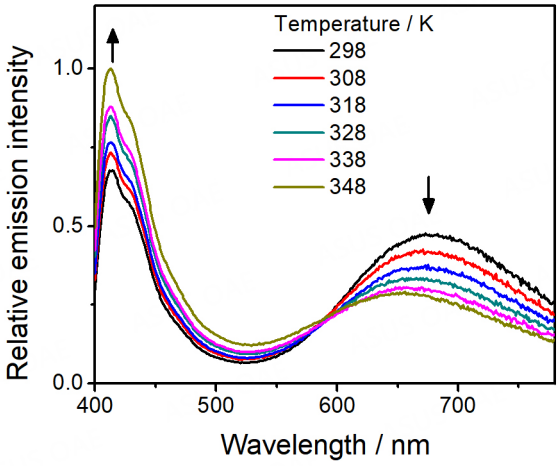

Figure 6. Emission spectra of [PF-{N_3C_2H-$C_6H_4C{\equiv}CPt(^tBu_3tpy)\}_2$](OTf)$_{2n}$ (**3**) in acetonitrile with increasing temperature.

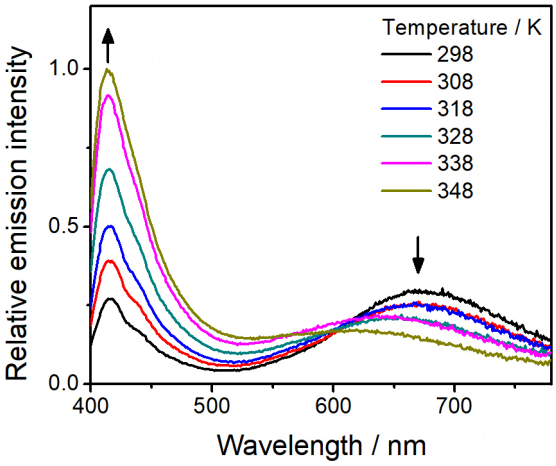

Figure 7. Emission spectra of [PFP-{N_3C_2H-$C_6H_4C{\equiv}CPt(^tBu_3tpy)\}_2$](OTf)$_{2n}$ (**4**) in acetonitrile with increasing temperature.

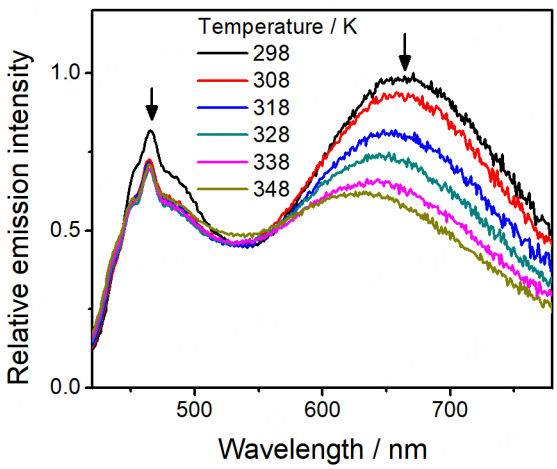

Figure 8. Emission spectra of [PFT-{N_3C_2H-$C_6H_4C{\equiv}CPt(^tBu_3tpy)\}_2$](OTf)$_{2n}$ (**5**) in acetonitrile with increasing temperature.

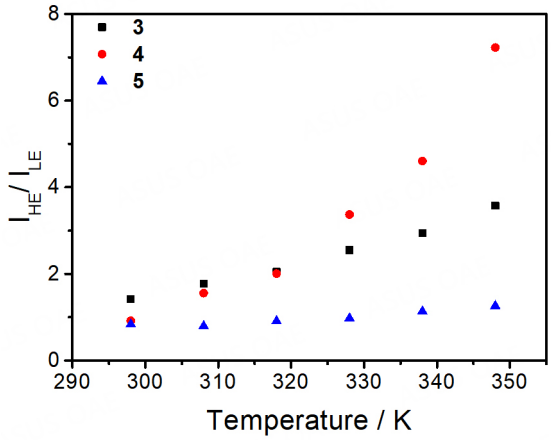

Figure 9. Ratiometric emission intensity plots of the high-energy (HE) and low-energy (LE) bands of **3**-**5** in acetonitrile with increasing temperature. I_{HE}/I_{LE} of **3** = I_{413nm}/I_{673nm}; I_{HE}/I_{LE} of **4** = I_{413nm}/I_{673nm}; I_{HE}/I_{LE} of **5** = I_{465nm}/I_{673nm}.

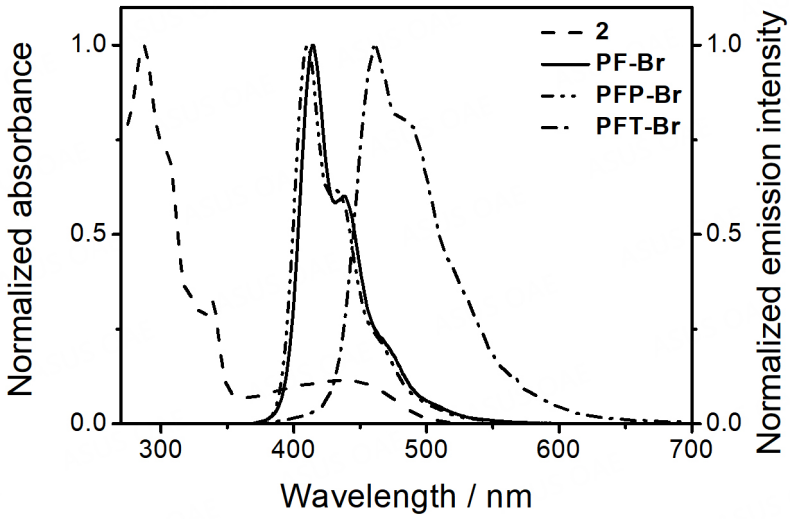

Figure 10. Normalized UV-vis absorption of [Pt(^{t}Bu$_3$tpy)(C≡CC$_6$H$_4$-C$_2$HN$_3$C$_6$H$_{13}$)]OTf (**2**) and emission spectra of **PF-Br**, **PFP-Br** and **PFT-Br** showing the spectral overlap between the emission spectra of the polymer energy donors and the UV-vis absorption spectrum of the platinum(II) complex **2** energy acceptor.

from the polymer backbone of **5** is found to be less effectively quenched when compared to that of **3** and **4**. The related parameters have been obtained and are summarized in Table 3. Since the platinum(II)-containing conjugated polymers **3**-**5** share similar molecular structures except for the polymer backbone, it is believed that the values of the relative orientation of the transition dipoles of the chromophores (κ) and the distance between the donor and the acceptor (r) should be almost the same. Therefore, the FRET efficiency is mainly governed by the emission quantum yield of the donor (Φ_D) and the spectral overlap integral of the absorption spectrum of the acceptor and emission spectrum of the donor ($J(\lambda)$), which are related to the Förster radius (R_0). It is found that the calculated R_0 value of **5** is the lowest, indicating that the FRET in **5** should be the least efficient, as reflected by the smallest decrease in emission quantum yield of the polymer backbone.

Table 3. Parameters obtained from the equation determining the Förster radius, R_0[a] of 3-5

Acceptor	Donor	Φ_D[b,c]	R_0/nm	Pt(II)-Polymer	Φ_{lum}[b,c,d]	Φ_{lum}/Φ_D
2	**PF-Br**	0.92	4.9	**3**	1.2×10^{-3}	1.30×10^{-3}
2	**PFP-Br**	0.90	4.9	**4**	9.0×10^{-4}	1.00×10^{-3}
2	**PFT-Br**	0.45	4.5	**5**	8.4×10^{-4}	1.87×10^{-3}

[a]$R_0 = 0.211[\kappa^2 n^{-4} \Phi_D J(\lambda)]^{1/6}$; [b]data obtained with an uncertainty of 10 %; [c]the relative luminescence quantum yields were measured at room temperature using quinine sulfate in 0.5 M H_2SO_4 as a standard; [d]the luminescence quantum yields of the polymer backbone.

CONCLUSION

Alkynylplatinum(II) terpyridine complexes (**1** and **2**) and alkynylplatinum(II) terpyridine-containing conjugated polymers with different polymer backbones (**3**-**5**) have been prepared, and their spectroscopic properties as well as FRET processes have been studied. The platinum(II)-containing polymers **3**-**5** are found to exhibit dual emissive features, in which the two emission bands correspond to ^{1}IL fluorescence from the polymer backbones and ^{3}MMLCT emissions from the platinum(II) pendants. Such unique luminescence behavior is attributed to the intramolecular Pt···Pt and/or π-π interactions between the platinum(II) pendants in the polymer molecules. The FRET processes between the conjugated polymer backbones and platinum(II) pendants have been studied systemically. It is found that **5** has the lowest Förster radii (R_0) among others, probably due to the lowest emission quantum yield of poly(fluorene-*co*-thiophene). Distinctive thermo-responsive ratiometric emission changes have been observed for **3** and **4**, in which an increase in intensity of the high-energy ^{1}IL emission originated from the polymer backbones and a decrease in intensity of the low-energy ^{3}MMLCT emission are found upon heating. The present work has demonstrated the utilization of "click" reaction for the convenient preparation of platinum(II)-containing conjugated polymers, which show unique photophysical and spectroscopic properties. Through the judicious design, ratiometric emission changes upon varying temperatures have been realized in this class of platinum(II)-containing polymers. This study may provide valuable insights into the preparation of metal-containing polymeric systems for different applications, such as thermochromic materials. Owing to the ease of structural modifications, various kinds of polymeric materials could be potentially fabricated, which could serve as thermochromic sensors for monitoring temperature in real time.

DECLARATIONS

Authors' contributions

Conducted the synthesis, characterization and photophysical measurements, analyzed the data and prepared the manuscript: Cheng HK

Initiated and designed the research, analyzed the data and prepared the manuscript: Yam VWW

Availability of data and materials

Not applicable.

Financial support and sponsorship

This work was supported by the Collaborative Research Fund (CRF) (C7075-21G) and the General Research Fund (GRF) from the Research Grants Council of the Hong Kong Special Administrative Region, People's Republic of China (HKU17303421), and the CAS-Croucher Funding Scheme for Joint Laboratory on Molecular Functional Materials for Electronics, Switching and Sensing. H.-K.C. acknowledges the receipt of a Postgraduate Studentship.

Conflicts of interest

All authors declared that there are no conflicts of interest.

Ethical approval and consent to participate

Not applicable.

Consent for publication

Not applicable.

REFERENCES

1. Burroughes JH, Bradley DDC, Brown AR, et al. Light-emitting diodes based on conjugated polymers. *Nature* 1990;347:539-41. DOI
2. Mcneill R, Siudak R, Wardlaw J, Weiss D. Electronic conduction in polymers. I. The chemical structure of polypyrrole. *Aust J Chem* 1963;16:1056-75. DOI
3. Bolto B, Weiss D. Electronic conduction in polymers. II. The electrochemical reduction of polypyrrole at controlled potential. *Aust J Chem* 1963;16:1076-89. DOI
4. Bolto B, Mcneill R, Weiss D. Electronic conduction in polymers. III. Electronic properties of polypyrrole. *Aust J Chem* 1963;16:1090-103. DOI
5. Mccullough RD. The chemistry of conducting polythiophenes. *Adv Mater* 1998;10:93-116. DOI
6. Sirringhaus H, Tessler N, Friend RH. Integrated optoelectronic devices based on conjugated polymers. *Science* 1998;280:1741-4. DOI PubMed
7. Ago H, Petritsch K, Shaffer MSP, Windle AH, Friend RH. Composites of carbon nanotubes and conjugated polymers for photovoltaic devices. *Adv Mater* 1999;11:1281-5. DOI
8. Friend RH, Gymer RW, Holmes AB, et al. Electroluminescence in conjugated polymers. *Nature* 1999;397:121-8. DOI
9. Sirringhaus H, Brown PJ, Friend RH, et al. Two-dimensional charge transport in self-organized, high-mobility conjugated polymers. *Nature* 1999;401:685-8. DOI
10. Mcgehee MD, Heeger AJ. Semiconducting (conjugated) polymers as materials for solid-state lasers. *Adv Mater* 2000;12:1655-68. DOI
11. Thomas SW 3rd, Joly GD, Swager TM. Chemical sensors based on amplifying fluorescent conjugated polymers. *Chem Rev* 2007;107:1339-86. DOI PubMed
12. Ho CL, Wong WY. Metal-containing polymers: facile tuning of photophysical traits and emerging applications in organic electronics and photonics. *Coord Chem Rev* 2011;255:2469-502. DOI
13. Gracia R, Mecerreyes D. Polymers with redox properties: materials for batteries, biosensors and more. *Polym Chem* 2013;4:2206. DOI
14. Liu S, Zhang K, Lu J, et al. High-efficiency polymer solar cells via the incorporation of an amino-functionalized conjugated metallopolymer as a cathode interlayer. *J Am Chem Soc* 2013;135:15326-9. DOI PubMed
15. Du M, Li C, Liu C, Fang S. Design and construction of coordination polymers with mixed-ligand synthetic strategy. *Coord Chem Rev* 2013;257:1282-305. DOI
16. Xu H, Chen R, Sun Q, et al. Recent progress in metal-organic complexes for optoelectronic applications. *Chem Soc Rev* 2014;43:3259-302. DOI PubMed
17. Winter A, Schubert US. Synthesis and characterization of metallo-supramolecular polymers. *Chem Soc Rev* 2016;45:5311-57. DOI PubMed
18. Ho CL, Yu ZQ, Wong WY. Multifunctional polymetallaynes: properties, functions and applications. *Chem Soc Rev* 2016;45:5264-95. DOI PubMed
19. Götz S, Zechel S, Hager MD, Newkome GR, Schubert US. Versatile applications of metallopolymers. *Prog Polym Sci* 2021;119:101428. DOI
20. Yu SC, Gong X, Chan WK. Synthesis and characterization of poly(benzobisoxazole)s and poly(benzobisthiazole)s with 2,2'-bipyridyl units in the backbone. *Macromolecules* 1998;31:5639-46. DOI
21. Chen X, Liao JL, Liang Y, Ahmed MO, Tseng HE, Chen SA. High-efficiency red-light emission from polyfluorenes grafted with cyclometalated iridium complexes and charge transport moiety. *J Am Chem Soc* 2003;125:636-7. DOI PubMed
22. Yam VWW, Wong KMC, Zhu N. Solvent-induced aggregation through metal···metal/π···π interactions: large solvatochromism of luminescent organoplatinum(II) terpyridyl complexes. *J Am Chem Soc* 2002;124:6506-7. DOI PubMed
23. Yam VWW, Chan KHY, Wong KMC, Zhu N. Luminescent platinum(II) terpyridyl complexes: effect of counter ions on solvent-induced aggregation and color changes. *Chem Eur J* 2005;11:4535-43. DOI PubMed

24. Yu C, Wong KMC, Chan KHY, Yam VWW. Polymer-induced self-assembly of alkynylplatinum(II) terpyridyl complexes by metal···metal/π···π interactions. *Angew Chem Int Ed* 2005;44:791-4. DOI PubMed
25. Yu C, Chan KHY, Wong KMC, Yam VWW. Single-stranded nucleic acid-induced helical self-assembly of alkynylplatinum(II) terpyridyl complexes. *Proc Natl Acad Sci USA* 2006;103:19652-7. DOI PubMed PMC
26. Leung SYL, Lam WH, Yam VWW. Dynamic scaffold of chiral binaphthol derivatives with the alkynylplatinum(II) terpyridine moiety. *Proc Natl Acad Sci USA* 2013;110:7986-91. DOI PubMed PMC
27. Wong KMC, Yam VWW. Luminescence platinum(II) terpyridyl complexes - From fundamental studies to sensory functions. *Coord Chem Rev* 2007;251:2477-88. DOI
28. Po C, Tam AYY, Wong KMC, Yam VWW. Supramolecular self-assembly of amphiphilic anionic platinum(II) complexes: a correlation between spectroscopic and morphological properties. *J Am Chem Soc* 2011;133:12136-43. DOI PubMed
29. Wong KMC, Yam VWW. Self-assembly of luminescent alkynylplatinum(II) terpyridyl complexes: modulation of photophysical properties through aggregation behavior. *Acc Chem Res* 2011;44:424-34. DOI PubMed
30. Cheung ASH, Leung SYL, Hau FKW, Yam VWW. Supramolecular self-assembly of amphiphilic alkynylplatinum(II) 2,6-bis(N-alkylbenzimidazol-2'-yl)pyridine complexes. *Chem Res Chin Univ* 2021;37:1079-84. DOI
31. Zheng X, Chan MHY, Chan AKW, et al. Elucidation of the key role of Pt···Pt interactions in the directional self-assembly of platinum(II) complexes. *Proc Natl Acad Sci USA* 2022;119:e2116543119. DOI PubMed PMC
32. Tam AYY, Wong KMC, Yam VWW. Unusual luminescence enhancement of metallogels of alkynylplatinum(II) 2,6-bis(N-alkylbenzimidazol-2'-yl)pyridine complexes upon a gel-to-sol phase transition at elevated temperatures. *J Am Chem Soc* 2009;131:6253-60. DOI
33. Yam VWW, Au VKM, Leung SYL. Light-emitting self-assembled materials based on d^8 and d^{10} transition metal complexes. *Chem Rev* 2015;115:7589-728. DOI PubMed
34. Yam VWW, Chan AKW, Hong EYH. Charge-transfer processes in metal complexes enable luminescence and memory functions. *Nat Rev Chem* 2020;4:528-41. DOI
35. Chan MHY, Yam VWW. Toward the design and construction of supramolecular functional molecular materials based on metal-metal interactions. *J Am Chem Soc* 2022;144:22805-25. DOI PubMed
36. Chan K, Chung CYS, Yam VWW. Conjugated polyelectrolyte-induced self-assembly of alkynylplatinum(II) 2,6-bis(benzimidazol-2'-yl)pyridine complexes. *Chem Eur J* 2015;21:16434-47. DOI PubMed
37. Chan K, Chung CYS, Yam VWW. Parallel folding topology-selective label-free detection and monitoring of conformational and topological changes of different G-quadruplex DNAs by emission spectral changes via FRET of mPPE-Ala-Pt(II) complex ensemble. *Chem Sci* 2016;7:2842-55. DOI PubMed PMC
38. Chan CWT, Chan K, Yam VWW. Induced self-assembly and disassembly of alkynylplatinum(II) 2,6-bis(benzimidazol-2'-yl)pyridine complexes with charge reversal properties: "proof-of-principle" demonstration of ratiometric förster resonance energy transfer sensing of pH. *ACS Appl Mater Interfaces* 2022;Online ahead of print. DOI PubMed
39. Sonogashira K, Takahashi S, Hagihara N. A new extended chain polymer, poly[trans-bis(tri-*n*-butylphosphine)platinum 1,4-butadiynediyl]. *Macromolecules* 1977;10:879-80. DOI
40. Takahashi S, Kariya M, Yatake T, Sonogashira K, Hagihara N. Studies of poly-yne polymers containing transition metals in the main chain. 2. Synthesis of poly[trans-bis(tri-*n*-butylphosphine)platinum 1,4-butadiynediyl] and evidence of a rodlike structure. *Macromolecules* 1978;11:1063-6. DOI
41. Beljonne D, Wittmann HF, Köhler A, et al. Spatial extent of the singlet and triplet excitons in transition metal-containing poly-ynes. *J Chem Phys* 1996;105:3868-77. DOI
42. Younus M, Köhler A, Cron S, et al. Synthesis, electrochemistry, and spectroscopy of blue platinum(II) polyynes and diynes. *Angew Chem Int Ed Engl* 1998;37:3036-9. DOI PubMed
43. Chawdhury N, Köhler A, Friend RH, et al. Evolution of lowest singlet and triplet excited states with number of thienyl rings in platinum poly-ynes. *J Chem Phys* 1999;110:4963-70. DOI
44. Rogers JE, Cooper TM, Fleitz PA, Glass DJ, Mclean DG. Photophysical characterization of a series of platinum(II)-containing phenyl−ethynyl oligomers. *J Phys Chem A* 2002;106:10108-15. DOI
45. Liu Y, Jiang S, Glusac K, Powell DH, Anderson DF, Schanze KS. Photophysics of monodisperse platinum-acetylide oligomers: delocalization in the singlet and triplet excited states. *J Am Chem Soc* 2002;124:12412-3. DOI PubMed
46. Schanze KS, Silverman EE, Zhao X. Intrachain triplet energy transfer in platinum-acetylide copolymers. *J Phys Chem B* 2005;109:18451-9. DOI PubMed
47. Clem TA, Kavulak DFJ, Westling EJ, Fréchet JMJ. Cyclometalated platinum polymers: synthesis, photophysical properties, and photovoltaic performance. *Chem Mater* 2010;22:1977-87. DOI
48. Thomas III SW, Yagi S, Swager TM. Towards chemosensing phosphorescent conjugated polymers: cyclometalated platinum(II) poly(phenylene)s. *J Mater Chem* 2005;15:2829. DOI
49. Wang P, Liu S, Lin Z, et al. Design and synthesis of conjugated polymers containing Pt(II) complexes in the side-chain and their application in polymer memory devices. *J Mater Chem* 2012;22:9576. DOI
50. Lu W, Law YC, Han J, et al. A dicationic organoplatinum(II) complex containing a bridging 2,5-bis-(4-ethynylphenyl)-[1,3,4]oxadiazole ligand behaves as a phosphorescent gelator for organic solvents. *Chem Asian J* 2008;3:59-69. DOI PubMed
51. Liu B, Yu W, Lai Y, Huang W. Blue-light-emitting fluorene-based polymers with tunable electronic properties. *Chem Mater*

2001;13:1984-91. DOI

52. Vamvounis G, Schulz GL, Holdcroft S. Enhanced blue-violet emission from poly(fluorene-*co*-thiophene) host-guest systems. *Macromolecules* 2004;37:8897-902. DOI
53. Grell M, Bradley DDC, Ungar G, Hill J, Whitehead KS. Interplay of physical structure and photophysics for a liquid crystalline polyfluorene. *Macromolecules* 1999;32:5810-7. DOI
54. Lim E, Jung B, Shim H. Synthesis and characterization of a new light-emitting fluorene-thieno[3,2-*b*]thiophene-based conjugated copolymer. *Macromolecules* 2003;36:4288-93. DOI